

From Concept to Realization: Designing Miniature Humanoids for Running

Youngbum Jun, Robert Ellenburg, and Dr. Paul Oh
Mechanical Engineering and Mechanics, Drexel University
Philadelphia, Pennsylvania, 19104, USA
yj55@drexel.edu, rwe24@drexel.edu, paul@coe.drexel.edu

ABSTRACT

Humanoid robots present exciting research possibilities such as human gaits, social interaction, and even creativity. Full-size humanoid designs have shown impressive capabilities, yet are custom-built and expensive. Cost and sophistication barriers make reproducing and verifying results very difficult. The recent proliferation of mini-humanoids presents an affordable alternative, in that smaller robots are cheaper to own and simpler to operate. At less than 2000 USD, these robots are capable of human-like motion, yet lack precision sensors and processing power. The authors' goal is to produce a miniature humanoid robot that is both small and affordable, while capable of advanced dynamic walking and running. This requires sensing of the robot's inertia and velocity, the forces on its feet, and the ability to generate and modify motion commands in real time. The presented design uses commercial parts and simple machining methods to minimize cost. A power-efficient mobile x86 computer on-board leverages existing operating systems and simplifies software development. Preliminary results demonstrate controlled walking and feedback control.

Keywords: ATLAS, Humanoids, ZMP, walking trajectory, ZMP compensator, landing control.

1. INTRODUCTION

Humanoids are bipedal robots that mimic human form and function. The Honda ASIMO and Sony QRIO are a couple examples of robots in human form and that have been choreographed to dance, play instruments and even conduct orchestras and public events. Such robots are impressive from an electro-mechanical perspective, but are cognitively challenged and hence cannot function autonomously. Other Humanoids constructed for research purposes include Waseda University's WABIAN [1], Tohoku University's MS DanceR (Mobile Smart Dance Robot) [2], and the KAIST Hubo [3]. However, these are highly customized and unique; which makes it difficult for others to validate, confirm and expand research hypotheses. Without wider-spread availability of such robots, progress in humanoid research remains slow with narrow impact. Mini-sized humanoids such as the Robonova and Bioloid have been commercially available since 2002. Since then, many research labs have utilized these systems for humanoid research. The robots themselves did not need to exactly mimic human behavior as the experiments mostly required limited motion and expression. Ellenburg et al. explored creative dance using the Robonova-1 [4]. In

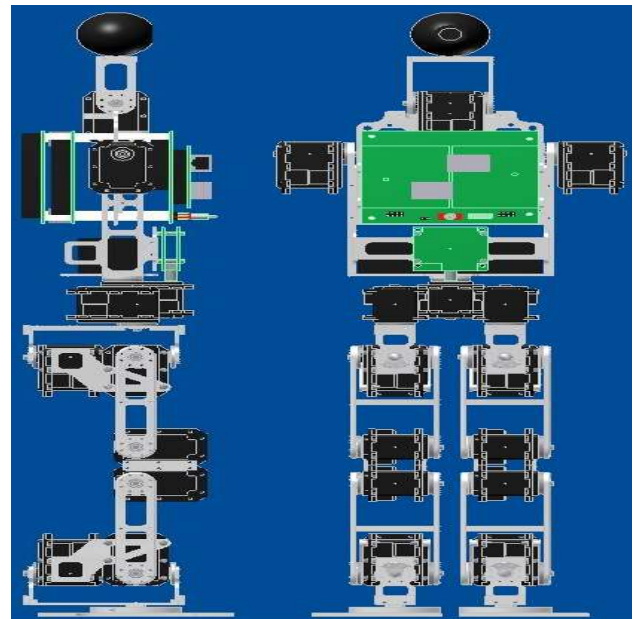


Fig. 1 CAD model of ATLAS humanoid showing board layout and servo locations.

[5] a Robonova was equipped with cameras using computer vision algorithms; it was able to perceptually interact with people.

Inexpensive commercial robots like the Robonova are limited in that they lack accurate sensors and position/torque feedback necessary for dynamic walking and running. To overcome such limitations, many research labs have designed their own miniature humanoid robots for research. Virginia Tech's DARwIn [6] uses off-the-shelf parts and an x86 processor running real-time LabVIEW to explore artificial intelligence and cooperative behavior. However, DARwIn and other humanoids of this form factor are limited by the low power-to-weight ratio of the robot servos. This severely limits the carrying capacity, and thus the size of computers and batteries that can fit onboard.

LabVIEW software is closed source, and costs thousands of dollars for a license. Although it simplifies hardware interfacing, it significantly adds to the cost of a research robot. Common realtime systems for Microsoft Windows such as RTX can cost as much as the robot itself.

With these ideas, we designed and constructed a mini-sized humanoid robot named ATLAS (DASL-1), which will competitively run in the July 2009 Robogames Humanoid 180-cm Dash event; competition for being the fastest humanoid robot in 180-cm straight line. A linear

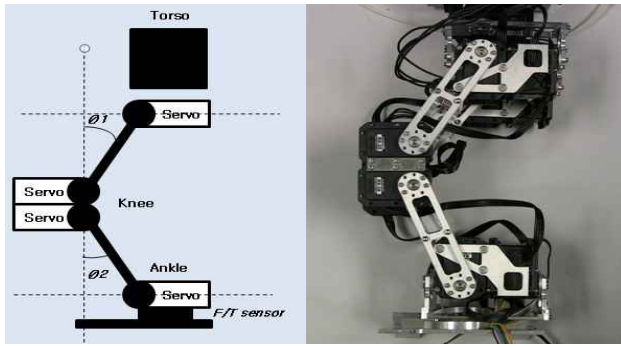


Fig. 2 Complimentary angle design of knee servos

inverted pendulum model based on Zero Moment point (ZMP) trajectory methods was used to estimate the dynamics and stability of ATLAS during running. Force-torque sensors (F/T sensor) and an Inertial Measurement Unit (IMU) was used to employ ZMP control algorithms during running.

Section 2 of this paper describes the mechanical design and system configuration of ATLAS. In section 3, a simple linear inverted pendulum model is demonstrated along with walking pattern generation, and walking control algorithms based on IMU and F/T sensors. Section 4 contains the experiment results with conclusions and future works in Section 5 and 6 respectively.

2. CONSTRUCTION OF A MINI-SIZED HUMANOID ROBOT

Mechanical design

We designed a mini-sized humanoid robot called ATLAS (Fig. 1) following these basic principles that inertia and mass consume energy to move, and running requires compliant joints for shock absorption and high joint speed/torque [7]. The mechanical design addressed these issues by minimizing the weight of brackets. Dynamixel RX-28 servos were used to move the robot. They were chosen both for their high power to weight ratio, and their software control of joint compliance. To minimize the weight of upper body, the actuation of the arms was reduced to 2 degrees of freedom (DOF) per arm. To reduce the moment of inertia, the battery and electronics were placed in the torso.

A key feature of the leg design is the double knee servo block as implemented previously in [8]. The knee joint must bend twice the angle of the hip and ankle joint to extend the leg. Two servos in the knee allow it to move at the same speed as the hip and ankle, removing this bottleneck (Fig. 2).

To pan and tilt a camera in the head, two additional DOF are needed. The camera can be panned side-to side with the torso twist, so a single head-tilt servo is used for the camera.

System design

Due to the small size of the robot, and the impacts and disturbances associated with running, the controller must update quickly to compensate. Additionally, more computational requirements are needed to process data generated simultaneously by sensors and for feedback at the same time. Since human operators must develop, test, and debug controllers and software, they need access to as much data about the robot's internal state as possible.

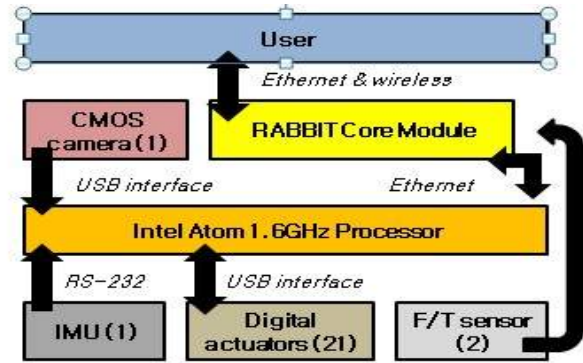


Fig. 3 System Architecture

Dimension		
Height	550 mm	
Width	150 mm	
Weight	3.1 kg	
Degree Of Freedom		
Legs	12 DOFs	
Arms	6 DOFs	
Waist	1 DOF	
Neck	1 DOF	
Total	20 DOF	
System	Descriptions	Specifications
Processor & board	Intel Atom Processor	1.6 GHz
	RABBIT core module	
	PC104 +	
Actuators	Dynamixel Rx-28	28.3 kg-cm holding torq.
Sensors	IMU	Gyro, Accelerometer
	Force-Torque sensor	
	CMOS Camera	320*240, up to 60f/sec
Battery	Li-Po	

Table. 1 System specification

The controller architecture and platform are shown in Fig. 3. It is based on x86 architecture and employs an Intel Atom 1.6 GHz processor board as a main controller with a PC104+ stack. Linux was chosen for the operating system because of its customizability and cost. A RABBIT core module is used to interface with two F/T sensors on the ankle, and it is connected to the main board through an Ethernet interface. Table.1 shows the overall system specification and mechanical dimension. To measure acceleration and angular momentum of the body, an IMU is placed on center of the pelvis, which directly sends data to the main board through an RS-232 interface. Communication between sensors and the computer is done through Ethernet. x86 architecture, Linux, and the Ethernet network offer high accessibility and simple expansion. The sensor-based feedback controls and USB interface between the actuators and processor guarantees real-time of motion.

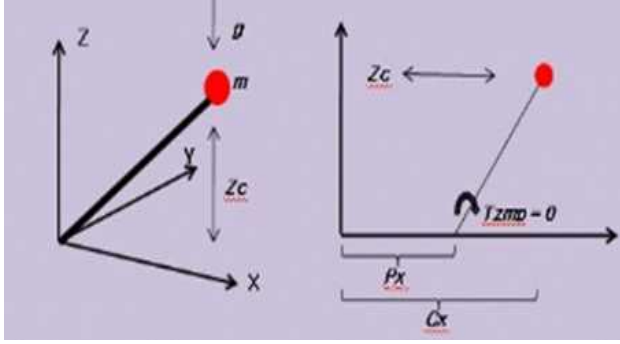


Fig. 4 Coordinate system of (a) 3D linear inverted pendulum mode, and (b) Zero moment point.

3. MOTION CONTROL SYSTEM

An important limitation of dynamic walking is stability control. One of the most popular approaches for stability of bipedal walking is Zero Moment Point (ZMP) Control. Approximating the body of the robot as a 3D linear inverted pendulum model [9, 10] simplifies dynamics of the humanoid. The ZMP is an imaginary point on the floor through which a pure force applied produces the desired hip acceleration [11]. An ideal inverted pendulum exerts a reaction force through the support rod, so the ZMP is by definition at the base of the pendulum. By approximating the supporting leg and hip as a pendulum, the ZMP is ideally kept in the center of the foot [10-13]. These simplified dynamics do not account for external disturbances, which cause the actual ZMP to deviate. To overcome this, many control algorithms were proposed such as ZMP compensator with inertia measurement [14, 18], ZMP preview control [15], and ZMP disturbance observer control [16].

The extensive research in ZMP control and trajectory generation is fertile ground for implementing walking control on a physical robot. Dealing with real world non-idealities will improve and expand on these control methods.

Dynamics and zero moment point

More specific dynamic equations produce better walking motion and stability with fewer controllers but requires more processing power to do so. Thus, a simple linear inverted pendulum is employed based on ZMP criterion to minimize the computational burden. Dynamics of ATLAS is based on a 3D Linear Inverted Pendulum Mode (3D-LIPM) shown in Fig. 4(a). XYZ is the global Cartesian coordinate and m is a point mass. The equations of motion of a 3D inverted pendulum model are non-linear. Under the assumptions of massless bar and the height of mass being constant, the equations of become the linear equation called 3D-LIPM [9-13] as shown below.

To derive the equation of motion for a 3D-LIPM, we assumed as follows [12-13]:

- 1) The height of mass is a constant.
- 2) The bar is massless.

Under the assumptions, the equation of motion of a 3D-LIPM is as follows:

$$\ddot{x} = \frac{g}{z_c} x + \frac{1}{m z_c} \tau_y \quad (1)$$

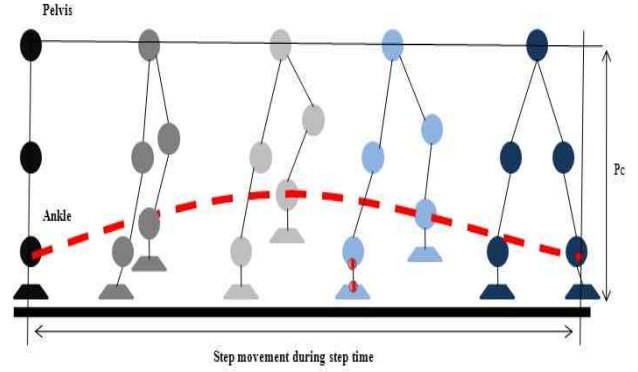


Fig. 5 Human foot trajectory

$$\ddot{y} = \frac{g}{z_c} y - \frac{1}{m z_c} \tau_x \quad (2)$$

Where m is the point mass of pendulum, z_c is the height of point mass, and g is the gravitational acceleration. τ_y and τ_x are the torque around y-axis and x-axis respectively.

Eq. (1) and Eq. (2) are linear and if we assume that no horizontal torques exist and the height of point mass is constant, we can derive ZMP equation from Eq. (1) and Eq. (2) [9-13].

$$p_y = c_y - \frac{z_c}{g} \ddot{c}_y \quad (3)$$

$$p_x = c_x - \frac{z_c}{g} \ddot{c}_x \quad (4)$$

Where p_x and p_y are ZMP in x-y plane and c_x and c_y are the coordinates of the point mass. Fig. 4(b) shows the definition of ZMP as an image. According to the definition of ZMP, the net moment at the pivot of the pendulum is zero, which means the torque generated by the reaction force due to the acceleration of the point mass is the same as the torque generated by the gravitational acceleration of the point mass as shown in Eq. 5 as below.

$$\tau_{zmp} = mg(c_x - p_x) - m c_x z_c = 0 \quad (5)$$

Walking trajectory generation

When people walk, they generate and change their trajectory in real-time based on circumstances. However, for robots the lack of computational speed and sensors makes it difficult to choose a walking pattern for non-ideal circumstances.

One approach to overcome this limitation is to define a walking trajectory for each situation the robot may encounter. For walking on even ground, feet and hip trajectory definitions are needed.

Foot trajectory: For human walking, the swing foot motion in the forward direction (x-direction) can be realized as a curvature as seen in Fig. 5 [14, 17]. This curvature can be defined simply as a cycloid function as follows:

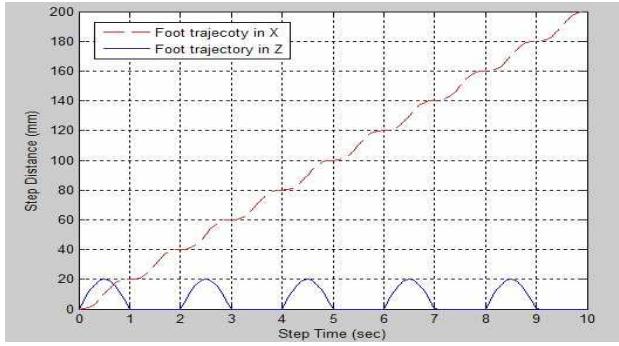


Fig. 6 Feet trajectory in global x and z axis

$$A_z(t) = h_z \sin\left(\frac{\pi}{S_t} t\right) \quad (6)$$

$$A_x = S_d \left(\frac{t}{S_t} - \frac{1}{2\pi} \sin\left(\frac{2\pi}{S_t} t\right) \right) \quad (7)$$

Where A_z and A_x are the ankle position in the z and x direction respectively, S_d and S_t are step distance and step time, respectively, and h_z is maximum height of ankle during step time. From Eq. (6) and Eq. (7), we can define the ankle trajectory in x and z direction shown in Fig. 6 as an example. In Fig. 6, the step time is set to 1 second, step distance is set to 20 mm per step time, and maximum height is set to 20 mm. Step time and step distance also determine the velocity and acceleration of the robot when walking, which yields the momentum of the robot. These parameters can be optimized through experiments.

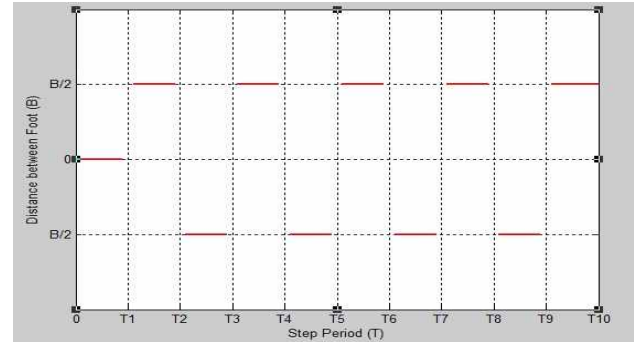
Hip trajectory: Hip trajectory is crucial for stable walking because it is assumed that the center of mass (COM) is located in the center of the pelvis. Hip trajectory should be extracted from the ZMP trajectory. In other words, a better ZMP trajectory yields better hip trajectory for stable walking. For stable walking, the ZMP should remain within the boundaries of a defined support polygon. Ideally this support polygon is defined on the sole of the robot's foot, which is a criterion widely used in biped robot research [9-13, 19]. With this idea, a reference ZMP trajectory in y and x direction is shown in Fig. 7. The T is the step period, D is the step distance, and B is the distance between the foot. These are defined through experiments.

When a reference ZMP trajectory is defined, the hip trajectory can be extracted using ZMP equations, Eq. (3) and Eq. (4) and solving the ODE initial value problem. By applying a Laplace transform to Eq. (3) and Eq. (4), we obtain the following [13].

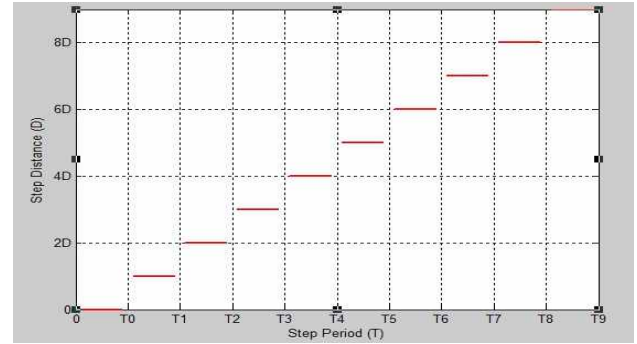
$$C_x(s) = \frac{1}{1 - \omega^2 s^2} (P_x(s) - \omega^2 C_x(0)s - \omega^2 \dot{C}_x(0)) \quad (8)$$

$$C_y(s) = \frac{1}{1 - \omega^2 s^2} (P_y(s) - \omega^2 C_y(0)s - \omega^2 \dot{C}_y(0)) \quad (9)$$

Where $\omega = \sqrt{\frac{z_c}{g}}$, z_c and g are previously defined in Eq. (1) and Eq. (2), C_x and C_y are the position of the center of mass in x and y direction respectively, and P_x and P_y are the ZMP in x and y direction respectively.



(a)



(b)

Fig. 7 (a) Prescribed ZMP trajectory in global Y direction and (b) in global X direction vs. step period.

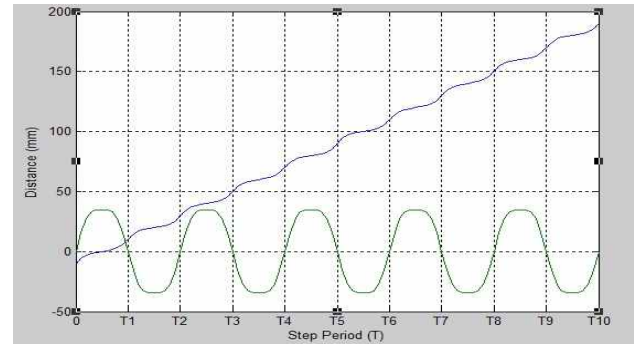


Fig. 8 reference hip trajectory in global X (slope) and Y (sinusoidal) direction when $A = 20\text{mm}$, $B = 20\text{mm}$.

To find ZMP in x and y-direction, $P_x(s)$ and $P_y(s)$, we apply Laplace transform to ZMP trajectories in Fig. 7 in x-direction and y-direction.

$$P_x(s) = 0 + \frac{Ae^{-T_0s}}{s} + \frac{Ae^{-2T_0s}}{s} + \frac{Ae^{-3T_0s}}{s} \dots \quad (10)$$

$$P_y(s) = 0 + \frac{1}{2} \frac{Be^{-T_0s}}{s} + \frac{Be^{-2T_0s}}{s} + \frac{Be^{-3T_0s}}{s} \dots \quad (11)$$

Where A is the step distance, B is the distance between the foot, and T_0 is the step time. From Eq. (8), (9), (10), (11), we can obtain the reference hip trajectory. Currently, these parameters are tweaked during experiments trials to maximize balance. Fig. 8 shows the hip trajectory derived from Eq. (8), (9), (10), (11) by applying an inverse Laplace transform.

K. Erbaturo et al. proposed the method to generate hip

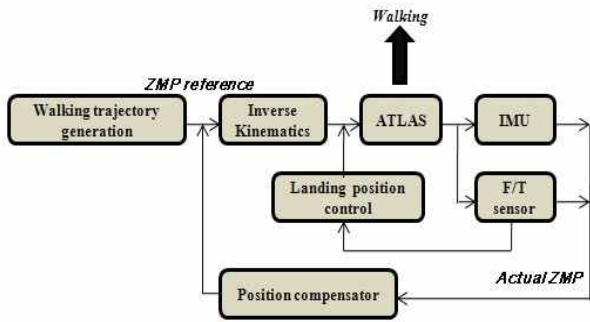


Fig. 9 Controller block diagram with all controllers active

trajectory based on ZMP trajectory by using Fourier series with inverse Laplace transform for periodic type walking motion. They simplified the hip trajectory as a function of Fourier series [13].

When the foot and hip trajectory are obtained in the time domain, all joint motions can be calculated using inverse kinematics.

Walking control

The stable ZMP trajectory calculations are based on a simplified model of the robot and specific walking conditions. During actual tests, the ZMP may be slightly different. To minimize the error and obtain high stability in walking, a ZMP compensator is employed based on IMU and F/T sensors. This compensates for any discrepancies in the model and various walking conditions and adjusts the position of the foot.

ZMP controller: Fig. 9 shows the control block diagram. The robot follows trajectories defined in the previous section. While the robot is moving, the IMU on the center of the pelvis measures the acceleration and angular moment of robot's body. The processor then calculates the difference between the current ZMP and the desired ZMP. All joint positions calculated using inverse kinematics based on the actual walking trajectory and are obtained in real time for a high stability margin. At the same time, the processor calculates the actual ZMP based on the ankle F/T sensors which measure reaction forces and torques on foot in the z-direction. A local coordinate system is placed on the foot with the origin being at the sole. Reaction forces are measured based on this coordinate system and the moment acting on the foot is calculated. By using the definition of ZMP criterion, the actual ZMP can be calculated using the moment of the foot. However, this data is used as a secondary control since the ZMP based on the F/T sensors is not always accurate.

Landing control: An important source of disturbance to the robot is the impact of the swing leg with the ground. Ideally, the collision of the foot occurs at prescribed time during the walk cycle. If the foot lands too soon or too late, the impact with the ground introduces unwanted impulses to the landing leg. The F/T sensors are used on each ankle to measure reaction force and moments at the foot. Since the reaction forces increase suddenly upon foot landing, these sensors allow the foot to measure when it touches the ground. This triggers the transition from single support to double support in the controller.

At different phases of walking, various controllers are turned on or off to control the hip and foot trajectories. By dividing the standard phases into discrete states, a

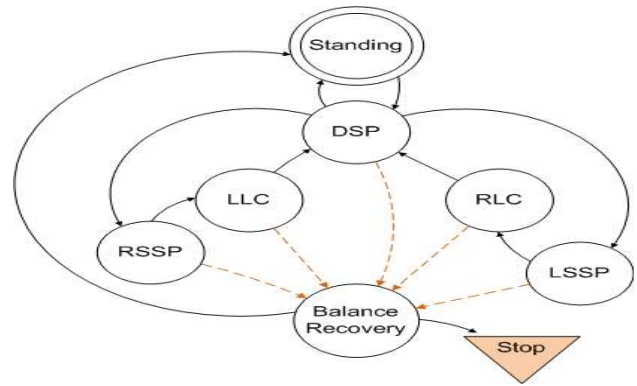


Fig. 10 State-flow diagram of walking pattern generation. This pattern forces the robot to start at double support, lift a foot and step, then control the foot's landing. If the IMU detects too much tilt, the robot tries to recover its balance, and resumes the pattern if possible.

simple switched-state controller (Fig. 10) can apply or remove different control techniques such as ZMP compensation and landing control only when they are appropriate. Controllers are enabled by adding their output together the walking trajectories or to the joint angles directly (Fig. 9).

4. EXPERIMENTAL RESULTS

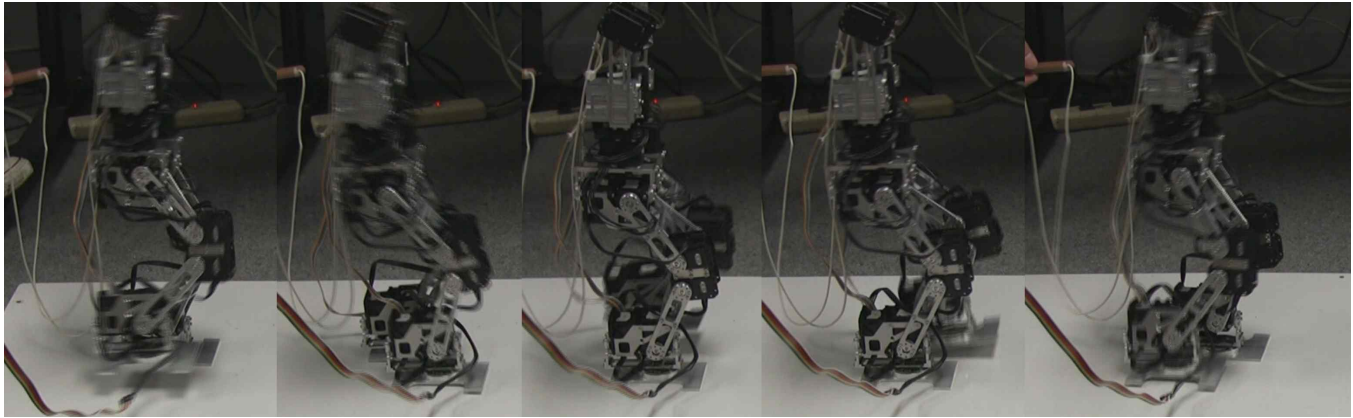
The most important issue in the dynamic walking is the stability of the open-loop dynamic walking. The robot cannot be controlled without the stability of the open-loop dynamic walking even if more sensors and control algorithms are employed. This section shows the open-loop stable dynamic walking of ATLAS.

By applying the approach presented previously, the stable trajectories were generated, and the parameters were defined through experiments. The image frames in Fig. 11 show the open-loop dynamic walking of ATLAS. Currently, the step time was 1 second and the step distance was 70 mm. The height of COM was 300 mm, the distance between the foot was 60 mm, and the maximum height of the foot trajectory was 40 mm. As a result, the velocity of ATLAS was 70 mm/second.

As the walking frequency and step size increased, however, the robot pitched and rolled with larger amplitude during the walk cycle until it could no longer stay stable. The open loop performance limit was partially addressed by feed-forward compensation, but only for the most basic disturbances such as knee deflection.

5. CONCLUSION

This paper presented a mini-sized humanoid named ATLAS, which has been in development since Jan. 2009. It was modeled using a simple 3D linear inverted pendulum with the ZMP criterion. The stable hip trajectory was generated through the fixed ZMP trajectory using Laplace Transform, and sinusoidal foot trajectory was defined mimicking the human walking. The IMU and F/T sensors were used to have more stability in the dynamic walking. The dynamic walking of ATLAS in Section 4 proved that the proposed design philosophy generates the stable dynamic walking for the mini-sized humanoid robots.



0.5 sec 1 sec 1.3 sec 1.6 sec 2 sec
Fig. 11 The dynamic walking of ALIAS in two seconds with two steps

6. FUTURE WORK

To improve the performance and stability of the robot, closed loop controllers designed for the robot will be implemented and proven in hardware. With the ability to accurately measure body position and ZMP, advanced techniques like variable ZMP trajectories [12, 13] can further reduce variations in the angular momentum of the robot's body and maximize forward velocity. By controlling the ZMP more directly, body accelerations required for high-speed turning and maneuvering become more controllable. Ultimately, the combination of inertial sensing and acceleration control will yield a robot capable of true running.

ACKNOWLEDGEMENTS

The authors would like to acknowledge Roy Gross for the mechanical design of ALIAS, Bob Sherbert for ALIAS programming and Bryan Kobe for sensor and circuit construction.

7. REFERENCE

[1] Ogura, Y.; Aikawa, H.; Shimomura, K.; Morishima, A.; Hun-ok Lim; Takanishi, A. "Development of a new humanoid robot WABIAN-2", *IEEE International Conference on Robotics and Automation (ICRA)*, pp.76-81, May 2006.
 [2] Kosuge, K.; Hirata, Y. "Human Robot Interaction", *IEEE International conference on Robotics and Biomimetics*, pp.8-11, August 2004.
 [3] Kim, J.H., Oh, J.H., "Walking Control of the Humanoid Platform KHR-1 based on Torque Feedback Control", *IEEE International Conference on Robotics and Automation (ICRA)*, Barcelona, Spain, April 2004.
 [4] Ellenberg, R., Grunberg, D., Kim, Y., Oh, P.Y., "Exploring Creativity through Humanoids and Dance", *5th International Conference on Ubiquitous Robots and Ambient Intelligence (URAI)*, Seoul, Korea, November 2008.
 [5] Maxwell, B.A. Leighton, B. Ramsay, A., "Development of Human-Robot Interaction System for Humanoid Robots", *5th International Conference on Ubiquitous Robots and Ambient Intelligence (URAI)*, Seoul, Korea, Nov 2008.
 [6] Muecke, M. and Hong, D. W., "The Synergistic Combination of Research, Education, and International Robot Competitions Through the Development of a Humanoid Robot", *32nd ASME Mechanisms and Robotics Conference*, New York City, NY, August 3-6, 2008.

[7] T. Yoshitsugu, T. Satoru, D. Shinich, and I. Akira, "Mechanical stress in knee joint during running at various speeds and step lengths", *Japanese Journal of Physical Fitness and Sports Medicine*, Vol. 53, No.1, pp.167-181, 2004
http://www.robots-dreams.com/2006/11/roboone_10_king.html
 [9] S. Kajita, F. Kanehiro, K. Kaneko, K. Yokoi, and H. Hirukawa, "The 3D linear inverted pendulum mode: A simple modeling for a biped walking pattern generation", in *Proc. IEEE/RSJ Int. Conf. Intell. Robots Syst.*, Oct. 29-Nov. 3 2001, vol.1, pp.239-246.
 [10] K. K. Noh, J. G. Kim, and U. Y. Huh, "Stability experiment of a biped walking robot with inverted pendulum", in *Proc. 30th Annu. Conf. IEEE IECON*, Nov.2-6, 2004, vol. 3, pp.2475-2479.
 [11] M. Vukobratovic, b. Borovac, "Zero-Moment Point-Thirty five years of its life", *International Journal of Humanoid Robotics*, vol.1 No.1, pp.157-173, 2004
 [12] C. Zhu, Y. Tomizawa, X. Luo, and A. Kawamura, "Biped Walking with Variable ZMP, Frictional Constraint, and Inverted Pendulum Model", *IEEE International Conference on Robotics and Biomimetics*, Shenyang, China, August 22-26 2004.
 [13] K. Erbatur, O. Kurt, "Natural ZMP Trajectories for Biped Robot Reference Generation", *IEEE Transactions on Industrial Electronics*, vol.56, No.3, March 2009.
 [14] I.W. Park, J.Y Kim, and J.H, Oh, "Online Biped Walking Pattern Generation for Humanoid Robot KHR-3(KAIST Humanoid Robot-3: Hubo)", *Humanoid Robots, 6th IEEE-RAS International Conference on*, pp.398-403, Dec 4-6 2006.
 [15] S. Kajita, F. Kanehiro, K. Kaneko, K. Fujiwara, K. Harada, K. Yokoi, and H. Hirukawa, "Biped walking pattern generation using preview control of the zero-moment-point", in *Proc, IEEE Int. Conf. Robot. Autom.*, Taipei, Taiwan, sep. 2003, vol. 2, pp.1620-1626
 [16] T. Sato, and K. Ohnishi, "ZMP Disturbance Observer for Walking Stabilization of Biped Robot", *10th IEEE International Workshop on Advanced Motion Control (AMC)*, pp.290-295, March 26-28, 2008
 [17] Q. Huang, K. Yokoi, S. Kajita, K. Kaneko, H. Arai, N. Koyachi, and K. Tanie, "Planning walking patterns for a Biped Robot", *IEEE Transactions on Robotics and Automation*, vol.17, No.3, June 2001.
 [18] Q. Li, A. Takanishi, and I. Kato, "A Biped Walking Robot Having A ZMP Measurement System Using Universal Force-Moment Sensors", *IEEE/RSJ International Workshop on Intelligent Robots and Systems (IROS)*, Osaka, Japan, Nov. 3-5, 1991.
 [19] Y. Choi, B.J. You, and S.R. Oh, "On the stability of indirect ZMP controller for biped robot systems", in *Proc. Int. Conf. Intell. Robots Syst.*, vol.2, pp.3-10, Sendai, Japan, Jun. 2004.